DALTON
FULL PAPER

Redox reactions of the boron subhalide clusters $B_nCl_n^{0/\cdot-/2-}$ (n = 8 or 9) investigated by electrochemical and spectroscopic methods †

Bernd Speiser,*[a] Carsten Tittel,[a] Wolfgang Einholz[b] and Ronald Schäfer[b]

[a] *Institut für Organische Chemie, Universität Tübingen, Auf der Morgenstelle 18, D-72076 Tübingen, Germany. E-mail: bernd.speiser@uni-tuebingen.de*
[b] *Institut für Chemie, Universität Hohenheim, Garbenstraße 30, D-70593 Stuttgart, Germany*

Received 23rd November 1998, Accepted 31st March 1999

The redox properties of the electron hyperdeficient boron subhalide clusters octachlorooctaborane(8), B_8Cl_8, and nonachlorononaborane(9), B_9Cl_9, were investigated in solution by cyclic voltammetry at platinum or glassy carbon electrodes, and by ^{11}B NMR as well as ESR spectroscopy. The neutral compounds undergo a spontaneous reduction by traces of moisture usually present even in dried solvents, and the voltammetric experiment starts from $B_8Cl_8^{\cdot-}$ or $B_9Cl_9^{\cdot-}$. The radical anions were identified by ESR spectroscopy. Their formation leads to line broadening in NMR spectra of B_nCl_n. Electrochemically, they are quasireversibly reduced to the dianions, but oxidized in an EC_{cat} (electrochemical step, catalytic chemical step) reaction with an essentially reversible electron transfer step to the neutral compounds. The potential ordering for the two redox processes is "normal" in both clusters, being in accordance with the fact that structural changes accompanying the electron transfer are minor. The radical anion $B_8Cl_8^{\cdot-}$ is even more stable against disproportionation than $B_9Cl_9^{\cdot-}$.

Introduction

Multiple-stage redox systems have extensively been studied in the case of organic (see, *e.g.* ref. 2) and organometallic (see, *e.g.* ref. 3) molecules. The spacing of the redox potentials for subsequent one-electron steps is an important factor which contributes to the behavior of compounds with several oxidation states.[4] Usually one would expect that oxidation or reduction becomes increasingly difficult with increasing or decreasing redox state of the molecule. It is thus common to find the difference in formal potentials in eqn. (1) for two-electron transfer

$$\Delta E^0 = E_2^0 - E_1^0 \quad (1)$$

reactions, eqns. (2) and (3), where the superscript for all species

$$A^0 \rightleftharpoons A^{1\pm} \pm e^- \; E_1^0 \quad (2)$$

$$A^{1\pm} \rightleftharpoons A^{2\pm} \pm e^- E_2^0 \quad (3)$$

indicates the difference in redox state relative to A^o ("+" for oxidations, "–" for reductions; often, but not always, the stable starting species is one of the "extreme" oxidation states, A^o or $A^{2\pm}$; A^o is not necessarily neutral) to be positive for oxidations and negative for reductions. The symbol $|\Delta E^0|$ will denote $E_2^0 - E_1^0$ for an oxidation and $-(E_2^0 - E_1^0)$ for a reduction. Then, the equilibrium (4) is characterized by an equilibrium constant

$$A^0 + A^{2\pm} \rightleftharpoons 2\,A^{1\pm} \quad (4)$$

in eqn. (5). In aprotic solvents $|\Delta E^0|$ often attains values of

$$K_{comp} = \frac{[A^{1\pm}]^2}{[A^0][A^{2\pm}]} = \exp\left[\frac{F}{RT}|\Delta E^0|\right] \quad (5)$$

approximately 0.4–0.5 V[4] ("normal potential ordering"). However, several examples have been identified where $|\Delta E^0|$ is decreased to values <0.4 V ("potential compression")[5] or the second electron transfer even occurs thermodynamically easier than the first one ("potential inversion").[6] In systems with potential inversion the intermediate redox state $A^{1\pm}$ is unstable with respect to disproportionation (4). Potential inversion is usually accompanied by a considerable change in the structure of the molecule during the redox process, for example conformational changes[1,7–10] or changes in cluster geometry.[11]

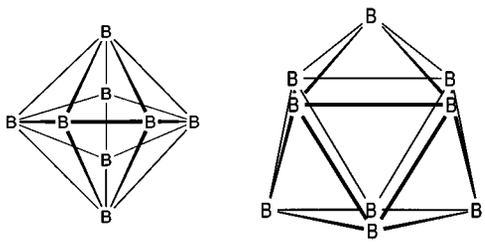

Fig. 1 Geometrical shapes of the deltahedral boron subhalide clusters B_nCl_n (n = 8 or 9).

One class of chemical compounds which could undergo two-electron transfers is the series of boron subhalide clusters with a 1 : 1 stoichiometry of boron *vs.* halogen. The chloroborane clusters B_nCl_n (n = 4, 8–12), of which B_8Cl_8 and B_9Cl_9 are investigated in this study, are classified as electron hyperdeficient molecules[12] and sometimes are called *hypercloso* clusters,[13] since the number of their framework electrons is 2n. The corresponding dianions *closo*-$B_nCl_n^{2-}$ (n = 6, 8–12) as well as the borate clusters *closo*-$B_nH_n^{2-}$ possess $2n + 2$ cage bonding electrons and follow Wade's rules of the framework electron count to structure correlation.[14] Nevertheless, the structures both of *hypercloso*-B_nCl_n (n = 8, 9) and *closo*-$B_nH_n^{2-}$ are based upon the same n-vertex deltahedra: dodecahedron (D_{2d} symmetry) for B_8Cl_8[15–17] and $B_8H_8^{2-}$,[18] tricapped trigonal prism (D_{3h} or C_{3v} symmetry, respectively) for B_9Cl_9[19,20] and $B_9H_9^{2-}$[21] (Fig. 1). For the system $B_9Br_9^{0/2-}$ it has recently been confirmed by X-ray crystallographic analysis and ELF (electron localization function) calculations[19] that the cluster structure remains intact upon the redox conversion while changes in atomic distances and bond angles occur. Such a behavior is in sharp contrast to

† Two-electron-transfer redox systems. Part 2.[1]

the structural rearrangements found during reduction of $[Os_6(CO)_{18}]$, which changes from a bicapped tetrahedral structure (neutral; $2n$ framework electrons) to an octahedron (dianion; $2n + 2$ framework electrons).[11] As well, the 6-vertex borate clusters $B_6X_6^{2-}$ (X = Cl, Br, I or H)[22–25] show the expected geometry of an octahedron, whereas the hypothetical neutral B_6H_6 is suggested by an *ab initio* study[26] to have a capped trigonal bipyramidal (bicapped tetrahedral) structure like $[Os_6(CO)_{18}]$. Furthermore, B_4Cl_4 molecules are tetrahedral with nearly T_d symmetry,[19,22,27] but the hypothetical $B_4H_4^{2-}$ ion is predicted by MNDO[28] and *ab initio* calculations[29] to exhibit a puckered D_{2d} conformation.

The reasons for these structural features can be traced to the degeneracy or non-degeneracy of the highest occupied (HOMO) and the lowest unoccupied (LUMO) molecular orbital of the polyhedrons:[30–32] the 8-vertex D_{2d} dodecahedron (B_8X_8 and $B_8X_8^{2-}$) and the 9-vertex D_{3h} tricapped trigonal prism (B_9X_9 and $B_9X_9^{2-}$) have non-degenerate frontier orbitals (HOMO and LUMO), and thus can accommodate, n, $n + 1$ or $n + 2$ framework electron pairs. In contrast, the HOMOs and LUMOs of most of the other *closo*-borates $B_nH_n^{2-}$ (n = 4–7, 10, 12) are degenerate. Removing two electrons from these clusters must result in a change of the structure according to Jahn–Teller theory.[33]

The ^{11}B NMR spectra of B_8Cl_8 and B_9Cl_9 do not show two different signals as would be expected by considering the molecular structure in the solid state, but only a single sharp resonance line ($\delta^{11}B$ 64.8 for B_8Cl_8 and 58.2 for B_9Cl_9, $h_{1/2} \approx 35$ Hz). This effect can be explained by the rapid fluctuation of these molecules in solution, which is described for the related eight-vertex cluster $B_8H_8^{2-}$ by the diamond–square–diamond transformation.[34] In contrast, the ^{11}B NMR spectrum of $B_9Cl_9^{2-}$ exhibits two peaks at δ −1.5 and −5.5 in an intensity ratio of 1:2 representing the three boron atoms with a connectivity of 4 and the six boron atoms with a connectivity of 5 in the cage.[19,35] Thus, there is no fluxional behavior or the transformation is very slow on the NMR timescale. The dianion of the eight-vertex polyhedron $B_8Cl_8^{2-}$ is not yet known in the literature. Since the corresponding hydrogen substituted cluster $B_8H_8^{2-}$, however, shows structural non-rigidity in solution, indicated by the appearance of only one ^{11}B NMR signal at room temperature ($\delta^{11}B$ −5.8, doublet, J_{B-H} = 128 Hz)[34,36] we could expect the same structural features for $B_8Cl_8^{2-}$.

In earlier work, B_9Cl_9 was reduced *chemically* to both its paramagnetic mono- and its di-anion, and $B_9Cl_9^{2-}$ oxidized by thallium(III) trifluoroacetate to the higher oxidation states.[35] Bowden[37] oxidized $B_9Cl_9^{2-}$ *electrochemically* in CH_2Cl_2 and CH_3CN, while Kellner[38] investigated the neutral B_9Cl_9 at a glassy carbon electrode in CH_2Cl_2.‡ In all cases, a stepwise redox reaction in the system $B_9Cl_9^{0/\bullet-/2-}$ was found, with all three redox states being stable in solution. The electron transfer chemistries of the smaller homologue B_8Cl_8 or its dianion do not seem to have been investigated.

Our results of a cyclic voltammetric and spectroscopic study of nonachlorononaborane(9), B_9Cl_9, and octachlorooctaborane(8), B_8Cl_8, are presented in this paper. Besides characterizing the redox chemistry of B_8Cl_8 for the first time, and determining the relative potential ordering of its formal potentials, we identified the starting species of the experiments to be different from B_nCl_n by means of rest potential measurements and ESR as well as NMR spectroscopy. Computer simulations of the cyclic voltammograms allowed the determination of kinetic constants.

‡ After finishing electrochemical experimental work for the present manuscript we became aware that similar cyclic voltammetric investigations of B_9Cl_9 but not B_8Cl_8 had been conducted at the Universität Stuttgart, Germany, and that a manuscript was being prepared by the groups involved. Preliminary manuscripts were exchanged in September 1998. We refer to this version of the Stuttgart manuscript,[39] which incorporates parts of the dissertation of Kellner.[38] Differences and similarities will be discussed in the course of the present paper.

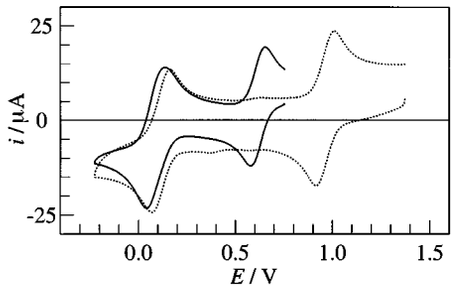

Fig. 2 Cyclic voltammograms of B_9Cl_9 (solid line) and B_8Cl_8 (dotted line) in CH_2Cl_2–0.1 M NBu_4PF_6 at a glassy carbon (GC) electrode with starting potentials located at values positive of both redox peak couples; $c^0(B_9Cl_9)$ = 1.7 mM, $c^0(B_8Cl_8) \approx 2$ mM, v = 0.2 V s^{-1}.

Results and discussion

Overall electrochemistry of B_nCl_n

Earlier cyclic voltammetric work with $B_9Cl_9^{2-}$ [37] and B_9Cl_9 [38,39] indicates that the redox states of the nonachlorononaborane(9) cluster can be converted in two stepwise one-electron transfers. Based on these results, we expected that B_9Cl_9, and in analogy also B_8Cl_8 would be stable at sufficiently positive electrode potentials E, and could be reduced to the respective dianions upon variation of E to less positive and finally negative values. Starting the voltammetric scan at rather positive potentials, both B_9Cl_9 and B_8Cl_8 in the dichloromethane electrolyte at Pt and glassy carbon (GC) electrodes indeed exhibit seemingly simple cyclic voltammograms with two separate peak couples (Fig. 2; the concentration of B_8Cl_8 used to record this voltammogram is only approximate due to some possible decay of the cluster during transfer to the cell). A close inspection of the current–potential curves, however, shows that at the starting potential of the voltammetric scan, where the B_nCl_n were expected to be stable, an appreciable oxidation current flows, even though the electrode is held at this potential for a "quiet time" of 10 s before the scan is actually initiated. This indicates that at the beginning of the experiment a species is present which can be oxidized at the rather positive starting potentials. It should be noted that published voltammograms of B_9Cl_9 and B_9Br_9 exhibit the same feature.[38,39]

The rest potential, E_{rest}, which is the potential at which no current flows through the working electrode in a particular electrolyte, provides a measure of the potential region where the initial species in the electrolyte is stable. Experimental determinations of E_{rest} in the B_nCl_n solutions immediately after dissolution of the neutral halides indeed result in values positive of the more anodic of the two peak couples in the voltammograms. However, E_{rest} is not stable and decreases to less positive values (Fig. 3). After some time a stable state is reached, with E_{rest} now located *between* the two peak couples of the respective voltammogram. Hence, the neutral clusters seem to undergo a reaction in the electrolyte to a product which is a less strong oxidant.

If the cyclic voltammetric starting potential is selected close to the steady-state value of E_{rest}, current–potential curves with a negligible current at E_{start} can be recorded for both clusters (Fig. 4). For the discussion below, only voltammograms recorded from such a starting potential were used. They show that the starting species is formed essentially quantitatively after dissolution and equilibration, and that it can be both oxidized and reduced in at least partially chemically and electrochemically reversible steps. In the case of B_9Cl_9 further, less intensive oxidation waves at more positive potentials were also observed. These will, however not be evaluated in the present paper.

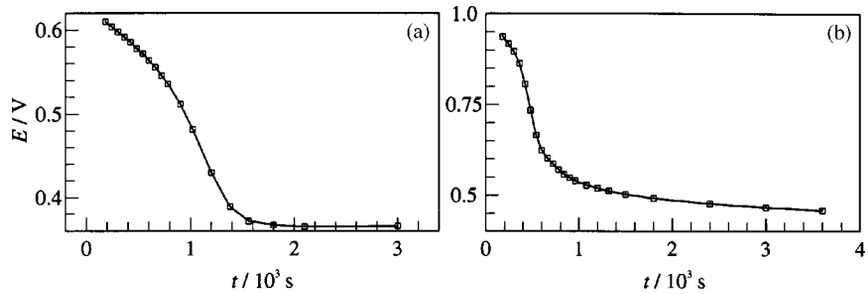

Fig. 3 Temporal development of the rest potential E_{rest} in solutions of B_9Cl_9 (a) and B_8Cl_8 (b) after dissolution at $t = 0$ s in CH_2Cl_2–0.1 M NBu_4PF_6 at a GC electrode; $c^0(B_9Cl_9) = 0.29$ mM, $c^0(B_8Cl_8) = 0.44$ mM.

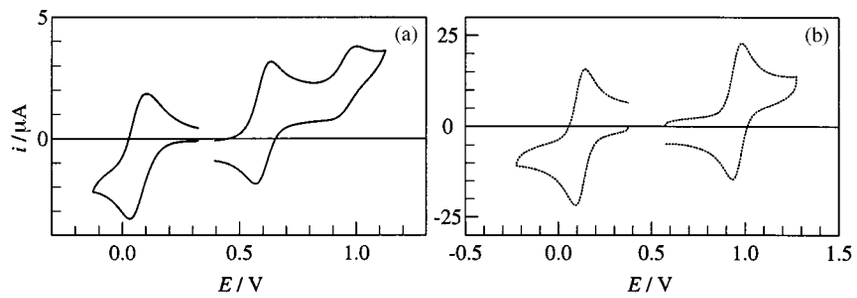

Fig. 4 Cyclic voltammograms of B_9Cl_9 [(a), $c^0 = 0.29$ mM, platinum electrode $v = 0.1$ V s^{-1}] and B_8Cl_8 [(b), $c^0 \approx 2$ mM, GC electrode, $v = 0.2$ V s^{-1}] in CH_2Cl_2–0.1 M NBu_4PF_6 with starting potentials located at steady-state value of rest potential.

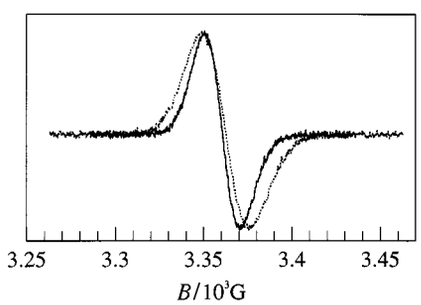

Fig. 5 The ESR spectra of solutions of B_9Cl_9 (solid line) and B_8Cl_8 (dotted line) in CH_2Cl_2–0.1 M NBu_4PF_6, 30 min after dissolution, assigned to $B_9Cl_9^{\bullet -}$ and $B_8Cl_8^{\bullet -}$ respectively.

Identification of starting species

For the interpretation of the voltammograms of the boron subhalide clusters it is essential to identify the starting species formed after dissolution of the neutral compounds. The fact that these species are stable at potentials between the two respective redox waves indicates that they might correspond to a compound with an oxidation state intermediate between those of B_nCl_n and $B_nCl_n^{2-}$, *i.e.* the radical anion $B_nCl_n^{\bullet -}$. Such a radical had been prepared in the case of the nine-vertex cluster by reduction of B_9Cl_9 with a stoichiometric amount of NBu_4I or oxidation of $B_9Cl_9^{2-}$ with thallium(III) trifluoroacetate and its ESR spectrum was reported with $g = 2.018$.[35] The neutral clusters, on the other hand, are diamagnetic.[40,41] The analogous B_9I_9 cluster undergoes one-electron reduction with organic donor solvents to form $B_9I_9^{\bullet -}$ within minutes, but was stable in chlorinated hydrocarbon solutions.[42] In contrast to earlier reports,[43] ESR signals were observed in BCl_3 solutions of B_8Cl_8 only with a very weak intensity or after addition of water, giving a different g value of 2.031, and were attributed to hydrolysis products.[40,41] The presence of $B_9Cl_9^{\bullet -}$ in the electrolyte after dissolution of B_9Cl_9 and equilibration is clearly shown by the ESR signal ($g = 2.018$, width 20 G, no hyperfine structure, Fig. 5) which is identical to the one reported earlier for the chemically prepared radical anion.[35]

In the case of B_8Cl_8 a similar ESR signal was found ($g = 2.017$, width 25 G, no hyperfine structure, Fig. 5). Proof that this ESR resonance is arising from the radical anion $B_8Cl_8^{\bullet -}$ follows from investigation of chemically prepared $NBu_4^+B_8Cl_8^{\bullet -}$ which shows the same ESR spectrum.

We thus conclude that B_9Cl_9 and B_8Cl_8 are reduced after dissolution in dichloromethane to their respective radical anions in a spontaneous redox process (6). The formation of $B_9Cl_9^{\bullet -}$ is

$$B_nCl_n + D \rightleftharpoons B_nCl_n^{\bullet -} + D^{\bullet +} \qquad (6)$$

observed in solutions of B_9Cl_9 in dichloromethane without supporting electrolyte to only a small extent, while the intensity of the ESR absorption is much stronger in the electrolyte containing NBu_4PF_6. After dissolution of B_9Cl_9 in the electrolyte, during ≈30 min a deepening of the solution color to brown is observed. Simultaneously, the ESR intensity increases. After this time the intensity of the ESR signals remains essentially constant, even upon standing overnight. Note that the timescale for this development of the color and the ESR intensity coincides with that of the rest potential variation (see Fig. 3).

Possibly, traces of moisture, coming either from the solvent, from the supporting electrolyte, or by diffusion of air into the electrochemical cell, are responsible for the formation of the radical anions $B_nCl_n^{\bullet -}$. We thus investigated solutions with various concentrations of B_8Cl_8 in carbon tetrachloride, chloroform, or dichloromethane with different contents of water by using dried and undried solvents. In each case we observed the ESR signal of $B_8Cl_8^{\bullet -}$. Only its intensity was varying depending on the contents of water. While in dried dichloromethane for example the intensity was low, it grew by a factor of about 15 after addition of undried, wet CH_3Cl_2. It is thus obvious that water is responsible for the formation of $B_8Cl_8^{\bullet -}$.

The corresponding ^{11}B NMR spectra of B_8Cl_8 solutions also reflect the influence of moisture on the half width and line shape of the B_8Cl_8 signal. When the dried solvent ($CDCl_3$ or CCl_4) and a relatively big amount of B_8Cl_8 was transferred to the NMR tube by means of vacuum or inert-gas techniques (concentration of $B_8Cl_8 \approx 0.03$ M), the ^{11}B resonance line was very sharp ($h_{1/2} \approx 35$ Hz at δ 64.8). When the NMR tube was opened to the atmosphere or when not well dried solvents were used the B_8Cl_8 signal was broadened ($h_{1/2} = 100$–200 Hz). This effect was even stronger when using CD_2Cl_2 ($h_{1/2} = 500$–1000

Hz). Line broadening of the NMR signal can be explained by a rapid exchange of an electron between the radical anion $B_8Cl_8^{\bullet -}$ and the neutral cluster.

When the concentration of B_8Cl_8 in dried CD_2Cl_2 was lower (0.003 M; closer to the situation as met in cyclic voltammetric experiments), no ^{11}B NMR resonance for B_8Cl_8 could be detected probably because B_8Cl_8 was nearly quantitatively reduced to the paramagnetic anion $B_8Cl_8^{\bullet -}$. Only an extremely weak signal at δ 58.2 (B_9Cl_9) was observed. This compound is probably present from the synthesis (see Experimental section). The intensity of the signal indicates that the concentration is so low that no peak in cyclic voltammograms should be visible.

For B_9Cl_9 a similar effect of line broadening in the ^{11}B NMR spectrum caused by traces of water was found. By adding an excess of BCl_3 under vacuum conditions the linewidth decreased. When NBu_4I was added in an equivalent amount to B_9Cl_9 the ^{11}B NMR signal disappeared. After condensing an excess of elemental bromine onto the mixture the sharp signal of B_9Cl_9 ($h_{1/2} \approx 50$ Hz) in the NMR spectrum reappeared. Thus, the overall reversibility of the redox process $B_9Cl_9 + e^- \rightleftharpoons B_9Cl_9^{\bullet -}$ is proven. Since it is obvious that traces of water are responsible for the formation of the radical anions $B_nCl_n^{\bullet -}$ ($n = 8$ or 9) we have to ask how this reduction process can occur. Water itself or in combination with the solvents CCl_4, $CHCl_3$ or CH_2Cl_2 can hardly act as an electron donor. Furthermore, there is no indication of a disproportionation of B_nCl_n leading to $B_nCl_n^{\bullet -}$ and $B_nCl_n^{\bullet +}$.

It is known that chloroborane clusters are cleaved by water to give $B(OH)_3$, HCl, and H_2.[43] We did not, however, observe any evolution of hydrogen. Since the redox potentials $E(B_nCl_n/B_nCl_n^{\bullet -})$ have rather high values (see Table 3), it could be expected that a neutral B_nCl_n molecule should be reduced instead of H^+. Since the voltammetric experiments show that most of the B_nCl_n molecules are reduced to the anions $B_nCl_n^{\bullet -}$ and because we could not find any other reaction products, it would be necessary that one molecule B_nCl_n reacts completely or nearly completely with the appropriate quantity of water according to eqn. (7), so that only a small amount of B_nCl_n will

$$B_nCl_n + 3n\,H_2O \longrightarrow n\,B(OH)_3 + 2n H^+ + n HCl + 2n e^- \quad (7)$$

$$B_nCl_n + e^- \longrightarrow B_nCl_n^{\bullet -}\ n = 8 \text{ or } 9 \quad (8)$$

be destroyed. At present, this hypothesis for the formation of the $B_nCl_n^{\bullet -}$ seems to be the most reasonable one, based on the experimental facts discussed above.

With this information we can explain the observations made during the reaction of B_8Cl_8 with CH_2Cl_2 which according to Morrison[44] and Emery[45] presumably gives the cluster molecules HB_9Cl_8, $H_2B_9Cl_7$, and B_9Cl_9. They noticed that the ^{11}B NMR spectrum does not show any resonance for B_8Cl_8 dissolved in dichloromethane. However, they found three signals at δ 70, 63.7, and 58.5 and assigned them to $H_2B_9Cl_7$, HB_9Cl_8, and B_9Cl_9, respectively along with a further signal at δ 40.25 (B–H). In contrast to this, in our NMR experiments, we never observed a signal at δ 40, which was supposed to indicate B–H groups. The other peaks we found as well when the least volatile fraction of B_8Cl_8 samples sublimed from the reaction mixture was used. The two downfield signals at δ 70 and 63.7 can be assigned to $B_{11}Cl_{11}$ ($\delta^{11}B$ 69.5[44]) and $B_{10}Cl_{10}$ ($\delta^{11}B$ 63.5[44]) since traces of these compounds together with B_9Cl_9 ($\delta^{11}B$ 58.2) are present in B_8Cl_8 samples before adding dichloromethane if B_8Cl_8 is not separated well from the by-products of its synthesis. Hence, we conclude that B_8Cl_8 is not reacting with CH_2Cl_2 to give the clusters HB_9Cl_8 and $H_2B_9Cl_7$, but that it is reduced to the paramagnetic radical anion $B_8Cl_8^{\bullet -}$ and this cannot be detected any more in the boron NMR spectrum. This result is in accordance with the cyclic voltammetric results, which indicate total disappearance of the neutral cluster upon dissolution in the electrolyte.

The spontaneous formation of $B_nCl_n^{\bullet -}$ from B_nCl_n also explains the result of a bulk electrolysis experiment with B_9Cl_9. If B_9Cl_9 were the starting species and were reduced to the stable $B_9Cl_9^{2-}$, 2 F were expected to be transferred upon reduction. Similarly, during reoxidation to B_9Cl_9 the charge should also correspond to 2 F. However, reduction used only ≈0.7 F, while reoxidation at +1.8 V results in the transfer of a much larger charge than expected. Taking into account some loss of B_9Cl_9 during transfer to the cell, the reduction charge thus indicates that only a one-electron step occurs, starting from $B_9Cl_9^{\bullet -}$ and leading to $B_9Cl_9^{2-}$. On the other hand, oxidation to B_9Cl_9 is followed by reaction (6) and reformation of the radical anion in a catalytic process (see also below, **Electrochemical oxidation of $B_nCl_n^{\bullet -}$**) and a large quantity of charge is transported through the electrolyte.

We thus conclude that the stable starting species present in the dichloromethane electrolyte is not B_nCl_n, but $B_nCl_n^{\bullet -}$ which can be reduced to $B_nCl_n^{2-}$ and oxidized to B_nCl_n in *heterogeneous* electron transfers at the electrode surface (Scheme 1);

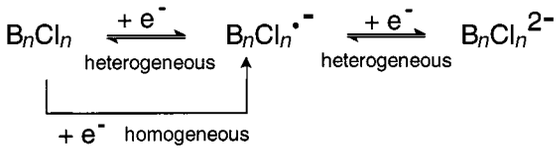

Scheme 1 Homogeneous and heterogeneous electron transfers in the system $B_nCl_n^{0/\bullet -/2-}$.

$B_nCl_n^{\bullet -}$ is formed from B_nCl_n in a *homogeneous* redox reaction (6). Since essentially all B_nCl_n is transformed into $B_nCl_n^{\bullet -}$, we can assume the concentration of the radical anion to be practically identical to the initial concentration of the neutral cluster. The loss of 5–6% due to reaction (7) can probably not be detected in electrochemical experiments, since it is within the conventionally assumed current measurement reproducibility of experiments such as those performed here.

Having established the starting species and the basic reaction steps of the $B_nCl_n^{0/\bullet -/2-}$ system in dichloromethane electrolyte, we will now separately discuss the determination of mechanistic, kinetic and thermodynamic parameters for the reduction and oxidation processes of the $B_nCl_n^{\bullet -}$ from electrochemical experiments.

Electrochemical reduction of $B_nCl_n^{\bullet -}$

Cyclic voltammograms and chronocoulograms of both B_9Cl_9 and B_8Cl_8 in CH_2Cl_2–0.1 M NBu_4PF_6 were recorded under variation of the concentration c^0 of the clusters and the scan rate v or pulse duration τ, respectively, in the potential range where reduction of the radical anions was observed. Both platinum and GC electrodes were used.

Cyclic voltammetry. Features of cyclic voltammograms from a typical series of experiments are given in Tables 1 and 2 for the reduction of the two boron subhalides. The peak potentials E_p^{red} and E_p^{ox} for the reduction and oxidation peak on the forward and reverse scans of the voltammograms, respectively, are essentially independent of the scan rate and the concentration. The peak potential difference ΔE_p is independent of v and close to 58 mV in all cases, indicating a situation close to electrochemical reversibility of the redox process. Independence of ΔE_p from c^0 demonstrates that compensation of the iR drop was effectively performed. The midpoint potential, $\bar{E}$, calculated as the mean value of the two peak potentials, is again independent of v and c^0. The electrochemical reversibility of the process is confirmed by the fact that the peak current function $i_p^{red}/\sqrt{v}c^0$ is independent of v and c^0. Furthermore, proportionality between i_p^{red} and the square root of the scan rate clearly indicates the absence of adsorption of electroactive species. Chemical reversibility, *i.e.* stability of the $B_nCl_n^{2-}$ species with respect to

Table 1 Typical cyclic voltammetric potential and current features for the reduction of $B_9Cl_9^{\bullet -}$ in CH_2Cl_2–0.1 M NBu_4PF_6 at a platinum electrode

c^0/mM	v/V s^{-1}	E_p^{red}/V	E_p^{ox}/V	ΔE_p/mV	$\bar{E}^a$/V	$i_p^{red}/\sqrt{v}c^{0\,b}$	i_p^{ox}/i_p^{red}
0.34	0.01	0.029	0.098	69	0.064	40.5	0.80
	0.02	0.028	0.097	69	0.063	38.9	0.98
	0.05	0.026	0.091	65	0.059	38.3	1.03
	0.1	0.027	0.091	64	0.059	40.8	1.00
	0.2	0.027	0.090	63	0.059	41.4	1.01
	0.5	0.028	0.091	63	0.060	39.2	1.05
	1.0	0.026	0.093	67	0.060	41.1	1.02
	2.0	0.026	0.096	70	0.061	41.4	1.02
	5.0	0.027	0.096	69	0.062	44.0	1.01
	10.0	0.025	0.092	67	0.059	44.0	1.04
0.67	0.01	0.031	0.098	67	0.065	38.9	0.94
	0.02	0.031	0.096	65	0.064	38.6	0.99
	0.05	0.029	0.095	66	0.062	38.6	1.00
	0.1	0.033	0.096	63	0.065	40.8	0.98
	0.2	0.031	0.097	66	0.064	40.8	0.98
	0.5	0.031	0.096	65	0.064	41.1	1.00
	1.0	0.029	0.097	68	0.063	41.1	1.00
	2.0	0.028	0.097	69	0.063	41.4	1.01
	5.0	0.031	0.097	66	0.064	42.0	1.08
	10.0	0.028	0.101	73	0.065	43.3	1.05
mean		0.029 ± 0.002	0.095 ± 0.003	67 ± 3	0.062 ± 0.002	40.8 ± 1.6	1.00 ± 0.06

^{a} Midpoint potential $\bar{E} = (E_p^{ox} + E_p^{red})2$. ^{b} In A cm^3 s$^{1/2}$ V$^{-1/2}$ mol^{-1}.

Table 2 Typical cyclic voltammetric potential and current features for the reduction of $B_8Cl_8^{\bullet -}$ in CH_2Cl_2–0.1 M NBu_4PF_6 at a platinum electrode

c^0/mM	v/V s^{-1}	E_p^{red}/V	E_p^{ox}/V	ΔE_p/mV	$\bar{E}^a$/V	$i_p^{red}/\sqrt{v}c^{0\,b}$	i_p^{ox}/i_p^{red}
0.21	0.01	0.082	0.144	62	0.113	32.3	0.99
	0.02	0.081	0.141	60	0.111	32.9	1.00
	0.05	0.079	0.144	65	0.112	33.5	1.03
	0.1	0.081	0.142	61	0.112	34.8	1.06
	0.2	0.079	0.141	62	0.110	34.8	1.02
	0.5	0.079	0.141	62	0.110	35.1	1.03
	1.0	0.079	0.143	64	0.111	35.4	1.02
	2.0	0.078	0.144	66	0.111	33.2	1.05
	5.0	0.076	0.140	64	0.108	33.2	1.06
	10.0	0.078	0.140	62	0.109	33.5	1.12
0.28	0.01	0.082	0.145	63	0.114	32.3	0.92
	0.02	0.083	0.144	61	0.114	32.3	0.98
	0.05	0.081	0.142	61	0.112	31.6	1.10
	0.1	0.084	0.143	59	0.114	33.2	1.02
	0.2	0.083	0.143	60	0.113	33.8	1.02
	0.5	0.081	0.144	63	0.113	34.2	1.02
	1.0	0.083	0.145	62	0.114	32.3	1.01
	2.0	0.083	0.147	64	0.115	32.3	1.04
	5.0	0.078	0.143	65	0.111	32.6	1.06
	10.0	0.080	0.147	67	0.114	32.9	1.12
mean		0.081 ± 0.002	0.143 ± 0.002	63 ± 2	0.112 ± 0.002	33.2 ± 0.9	1.03 ± 0.05

^{a} Midpoint potential $\bar{E} = (E_p^{ox} + E_p^{red})/2$. ^{b} In A cm^3 s$^{1/2}$ V$^{-1/2}$ mol^{-1}.

follow-up reactions, is indicated by the values of i_p^{ox}/i_p^{red}, which are close to 1.0. Only at scan rates below 0.02 V s^{-1} the value of this ratio drops below unity. Under the experimental conditions of this work this could be due to some non-linear diffusion ("edge") effects, which become increasingly important at slow scan rates. Also, additional transport by convection may play a role. The peak currents at scan rates above 0.02 V s^{-1}, however, allow the determination of the diffusion coefficient of $B_nCl_n^{\bullet -}$ in the electrolyte used for the experiments.[46]

The midpoint potentials for reduction and the diffusion coefficients of $B_9Cl_9^{\bullet -}$ and $B_8Cl_8^{\bullet -}$ are given in Table 3 as mean values from several independent experiments. All values are independent of the electrode material used. The standard deviations of the $\bar{E}$ results show excellent reproducibility comparable to that within individual experiments (Tables 1 and 2). On the other hand, while $i_p^{red}/\sqrt{v}c^0$ is excellently reproducible within a series of experiments in a single cell set-up, even with variation of the concentration (Tables 1 and 2), the diffusion coefficients vary more strongly between set-ups. These variations may be due to problems with the determination of c^0 and the limited stability of the neutral boron cluster starting compounds. The diffusion coefficient of the B_8Cl_8 species, however, appears consistently higher than that of the larger B_9Cl_9 species.

Table 3 Midpoint potentials $\bar{E}$ and diffusion coefficients D describing electrochemical reduction and transport of $B_nCl_n^{0/\bullet -/2-\,a}$

Redox process	$\bar{E}$/V	10^6 D/cm^2 s^{-1}
$B_9Cl_9^{\bullet -} + e^- \rightleftharpoons B_9Cl_9^{2-}$	+0.064 ± 0.003	2 ± 2 ^{b}
		2 ± 1 ^{c}
$B_9Cl_9^{\bullet -} \rightleftharpoons B_9Cl_9 + e^-$	+0.599 ± 0.003	1 ± 1 ^{b}
		1 ± 1 ^{c}
$B_8Cl_8^{\bullet -} + e^- \rightleftharpoons B_8Cl_8^{2-}$	+0.114 ± 0.002	4 ± 1 ^{b}
		3 ± 2 ^{c}
$B_8Cl_8^{\bullet -} \rightleftharpoons B_8Cl_8 + e^-$	+0.959 ± 0.002	4 ± 1 ^{b}
		4 ± 2 ^{c}

^{a} Mean values from several independent experiments under variation of scan rate v, concentration c^0, and electrode material. ^{b} From cyclic voltammograms. ^{c} From chronocoulograms.

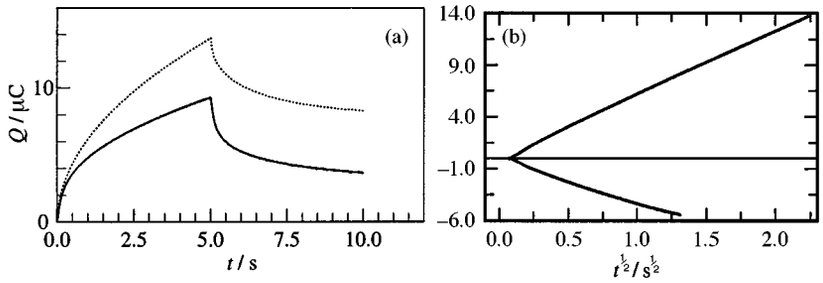

Fig. 6 (a) Chronocoulograms for the reduction of $B_9Cl_9^{\bullet -}$ (solid line) and $B_8Cl_8^{\bullet -}$ (dotted line) in CH_2Cl_2–0.1 M NBu_4PF_6, $\tau = 10$ s, GC electrode; $c^0(B_9Cl_9) = 0.29$ mM, $c^0(B_8Cl_8) = 0.44$ mM. (b) Anson plot for reduction of $B_8Cl_8^{\bullet -}$; "time$^{1/2}$" axis corresponds to $t^{1/2}$ for the forward part (upper trace) and $\tau^{1/2} + (t - \tau)^{1/2} - t^{1/2}$ for the reverse part (lower trace) of the chronocoulometric experiment.

Table 4 System parameter[a] sets used for simulations of the process $B_nCl_n^{\bullet -} + e^- \rightleftharpoons B_nCl_n^{2-}$

Parameter	$n = 9$	$n = 8$
E^0/V	+0.067	+0.112
10^6 D/cm^2 s^{-1}	1	4
k_s/cm s^{-1}	0.015	0.05
α	0.5	0.5

[a] Parameters describing the details of the mechanistic reaction steps.[49]

Chronocoulometry. The cyclic voltammetric data were complemented with chronocoulometric results (Fig. 6). Chronocoulometry confirms the electrochemical and chemical reversibility of the reduction of the radical anions by the almost linear plots of Q *vs.* $t^{1/2}$ ["Anson plots"; Fig. 6(b)][47] and the charge ratio[48] $Q_{2\tau}/Q_\tau = 0.41 \pm 0.03$ for $B_9Cl_9^{\bullet -}$ (τ is the pulse time, *i.e.* the time when the potential during the chronocoulometric experiment is switched). In the case of $B_8Cl_8^{\bullet -}$, $Q_{2\tau}/Q_\tau$ is slightly larger (0.63 ± 0.04) than the expected value of 0.41, but does not increase with increasing pulse time. In accordance with the interpretation of the cyclic voltammetric data, we thus exclude a chemical follow-up reaction of $B_8Cl_8^{2-}$. The Anson plots do show only a negligible intersection with the charge axis, thus confirming that none of the redox species is adsorbed at either electrode material used.

From the slopes of the Anson plots values of the diffusion coefficients are calculated in good agreement with the results of cyclic voltammetry, but again with rather high standard deviations. The mean values from several independent experiments are given in Table 3.

Simulation. The information determined from these quantitative analyses of cyclic voltammograms and chronocoulograms was subsequently used as the basis for simulations of the experimental current–potential curves. A simple quasi-reversible one-electron transfer under planar diffusion conditions was assumed as the mechanistic model of the reduction. For each of the compounds a single set of system parameters (formal potential E^0, diffusion coefficient D, heterogeneous electron transfer rate constant k_s, and transfer coefficient, α; Table 4) was sufficient to simulate various series of voltammograms at different v, c^0 and electrode material. This set was found by varying E^0, D, and k_s, until an optimum fit was obtained. The diffusion coefficients of the respective neutral, mono- and di-anionic species were assumed to be identical. The value of α was fixed in the calculations to 0.5 for both compounds. Variation of α did not significantly improve the fits.

Comparisons of the simulations to the corresponding experimental curves for both B_nCl_n at various scan rates and a single c^0 are shown in Fig. 7. The fit between theory and experiment is excellent, except for the smallest scan rate used, where possibly non-ideal transport effects are already visible in the experimental data. Thus, the simulations confirm the qualitative mechanistic picture gained so far. Also, the parameters E^0 and D obtained from the fitting procedure compare very well to the midpoint potentials $\bar{E}$ and diffusion coefficients determined before. For both the nine and the eight vertex cluster, values of k_s close to the limit of electrochemical reversibility ($k_s \approx 0.1$ cm s^{-1})[50] were found.

Electrochemical oxidation of $B_nCl_n^{\bullet -}$

In analogy to their reduction, the anodic oxidation of the B_nCl_n radical anions was investigated in CH_2Cl_2–0.1 M NBu_4PF_6.

Cyclic voltammetry. Cyclic voltammetric results for the oxidation of the $B_nCl_n^{\bullet -}$ to the B_nCl_n are collected in Tables 5 and 6. Only the first oxidation of $B_9Cl_9^{\bullet -}$ was analysed, and the switching potential for the voltammograms was adjusted accordingly. As in the case of the reduction of the $B_nCl_n^{\bullet -}$, the peak potential features for the oxidation clearly indicate a one-electron process close to electrochemical reversibility. Both the oxidation and the reduction peak potentials are independent of c^0 and v; the peak potential difference is independent of these experimental parameters and close to the reversible limit of 58 mV. Also, the midpoint potential does not depend either on the experimental parameters or on the electrode material used (Pt or GC; for the mean values from several independent experiments see Table 3).

On the other hand, the peak current data show that, at least at slow scan rates, some additional chemical reaction of B_nCl_n must take place: for $v \leq 0.02$ V s^{-1} the peak current function $i_p^{ox}/\sqrt{v}c^0$ starts to increase, but, moreover, i_p^{red}/i_p^{ox} clearly decreases to values below 1.0 for $v \leq 0.5$ ($B_9Cl_9^{\bullet -}$) or ≤ 0.2 V s^{-1} ($B_8Cl_8^{\bullet -}$). Computer simulations of the cyclic voltammograms (see below) show that the homogeneous conversion of B_nCl_n into $B_nCl_n^{\bullet -}$ can explain this behavior.

The interpretation of these features of the current–potential curves is hampered by the fact that at scan rates above $v = 1$ V s^{-1} the reproducibility of the peak current data decreases. Also, in this experimental time regime the background correction leads to artifacts, in particular at the beginning of the voltammetric scan and close to the switching potential. These problems were much more severe for the octaboron cluster as compared to the B_9Cl_9 system, and also more pronounced for GC as compared to Pt as the electrode material. For these reasons, only data from the limited range of scan rates $0.01 \leq v \leq 1$ V s^{-1} were evaluated. Here, however, mean values of the voltammetric potential features are reproducible both within an experiment and within several sets of cell set-ups (Tables 5 and 6, as well as Table 3, respectively). The mean values of the diffusion coefficients as derived from the oxidation peak currents over all independent experiments are also given in Table 3. Similar reasons as given in the case of reduction of the radical anions explain the relatively high standard deviations.

Chronocoulometry. Chronocoulometric oxidations of the $B_nCl_n^{\bullet -}$ cluster species met similar problems as those in the cyclic voltammetric experiments. In particular, shortly after switching back the potential ($t \geq \tau$), distortions of the charge *vs.* time curves were observed. For pulse lengths longer than

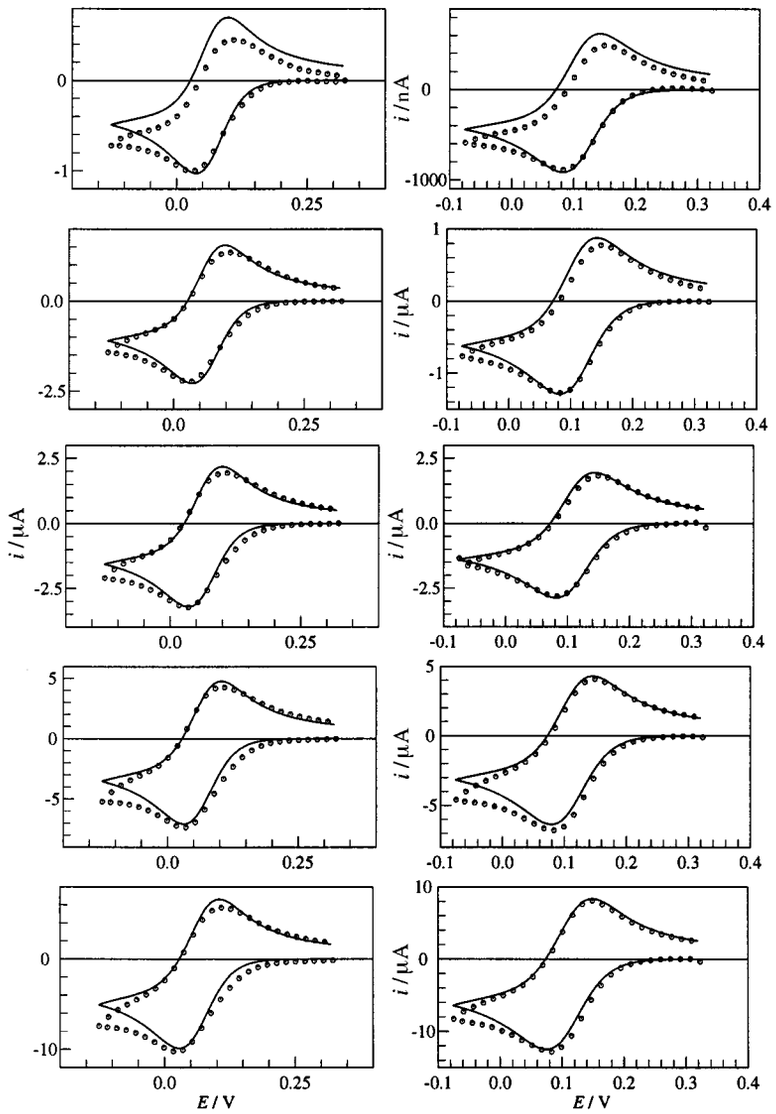

Fig. 7 Simulated (solid lines) and experimental (dots) cyclic voltammograms for the reduction processes of $B_9Cl_9^{\bullet -}$ (left; $c^0 = 0.63$ mM, Pt, $v = 0.01, 0.05, 0.1, 0.5, 1.0$ V s^{-1}, from top to bottom) and $B_8Cl_8^{\bullet -}$ (right; $c^0 = 0.28$ mM, Pt, $v = 0.01, 0.02, 0.1, 0.5, 2.0$ V s^{-1}).

several s, however, still reasonably linear Q *vs.* $t^{1/2}$ plots were obtained with negligible intersections with the charge axis. We exclude adsorption of electroactive material at the electrode surface also for the oxidation process of the cluster radical anions. The slopes of these plots were evaluated in order to estimate values for the diffusion coefficients, and again the results are presented in Table 3.

Simulation. The cyclic voltammetric curves of the oxidation processes leading from the boron subhalide radical anions to their neutral redox partners were simulated starting from the parameters determined as discussed in the previous paragraphs (Fig. 8). In this case a more complex reaction model than a simple quasireversible electron transfer was used. We retained the assumption of planar diffusion. However, the homogeneous redox process converting B_nCl_n produced at the electrode back to $B_nCl_n^{\bullet -}$ was added to the one-electron oxidation ("catalytic" follow-up reaction; EC_{cat} mechanism[46,51,52]). Values of E^0, D, k_s, and the rate constant k for the homogeneous electron transfer step were varied until an optimum fit between experiment and theory was found for $0.01 \leq v \leq 10$ V s^{-1} and two concentrations of $B_nCl_n^{\bullet -}$. The homogeneous step was assumed to follow first-order kinetics in this model. Again, $\alpha = 0.5$ was used throughout. Close to the switching potential the fit between experimental and simulated curves is less satisfactory as compared to that for the reductive voltammograms discussed before. However, the changes in the shapes of the voltammograms at slow scan rates (decrease of reverse peak intensity, flattening of forward peak) which are characteristic for the EC_{cat} mechanism[46,51,52] are modelled adequately. Table 7 lists the optimum values of the system parameters as found from the best fitting simulations. The results for the E^0 compare excellently to the $\bar{E}$ determined from the peak potential analysis (Table 3). The diffusion coefficients for the particular B_9Cl_9 experiments evaluated in the simulation are somewhat smaller than the mean values in Table 3, but we again attribute this to the low reproducibility of the concentration owing to the reactivity of the starting material.

In the case of the $B_9Cl_9^{\bullet -}$ oxidation the fitting procedure of DigiSim converged on a value of 1400 cm s^{-1} for the heterogeneous electron transfer rate constant. This indicates that the electron transfer is indeed fully diffusion controlled, *i.e.* electrochemically reversible. The numerical value, however, is not regarded as significant, since at such large rate constants the features of the cyclic voltammograms do no longer change with k_s, and, consequently, the sensitivity of the curves with respect to this parameter becomes close to zero.[53] The fitting routine will select a numerical value for this parameter which is strongly influenced by random errors in the data and is expected to have a large statistical uncertainty.[54] The DigiSim software does not

Table 5 Typical cyclic voltammetric potential and current features for the oxidation of $B_9Cl_9^{\bullet -}$ in CH_2Cl_2–0.1 M NBu_4PF_6 at a platinum electrode

c^0/mM	v/V s^{-1}	E_p^{ox}/V	E_p^{red}/V	ΔE_p/mV	$\bar{E}^a$/V	$i_p^{ox}/\sqrt{v}c^{0\,b}$	i_p^{red}/i_p^{ox}
0.34	0.01	0.629	0.560	69	0.595	42.4	0.62
	0.02	0.627	0.563	64	0.595	37.3	0.81
	0.05	0.630	0.561	69	0.596	39.5	0.85
	0.1	0.628	0.565	63	0.597	37.3	0.93
	0.2	0.628	0.565	63	0.597	37.9	0.94
	0.5	0.628	0.565	63	0.597	36.7	0.99
	1.0	0.631	0.562	69	0.597	36.0	1.01
	2.0	0.629	0.561	68	0.595	—	—
	5.0	0.628	0.561	67	0.595	—	—
	10.0	0.631	0.560	71	0.596	—	—
0.67	0.01	0.629	0.559	70	0.594	40.5	0.60
	0.02	0.627	0.561	66	0.594	37.6	0.74
	0.05	0.628	0.564	64	0.596	35.7	0.86
	0.1	0.627	0.565	62	0.596	37.0	0.87
	0.2	0.627	0.568	59	0.598	35.1	0.93
	0.5	0.628	0.567	61	0.598	35.1	0.97
	1.0	0.630	0.566	64	0.598	34.5	0.98
	2.0	0.630	0.565	65	0.598	—	—
	5.0	0.627	0.563	64	0.595	—	—
	10.0	0.630	0.558	72	0.594	—	—
mean		0.628 ± 0.001	0.563 ± 0.003	66 ± 2	0.596 ± 0.001	36.6 ± 1.4[c]	—

[a] Midpoint potential $\bar{E} = (E_p^{ox} + E_p^{red})/2$. [b] In A cm^3 s$^{1/2}$ V$^{-1/2}$ mol^{-1}. [c] From values for $v > 10$ mV s^{-1}.

Table 6 Typical cyclic voltammetric potential and current features for the oxidation of $B_8Cl_8^{\bullet -}$ in CH_2Cl_2–0.1 M NBu_4PF_6 at a platinum electrode

c^0/mM	v/V s^{-1}	E_p^{ox}/V	E_p^{red}/V	ΔE_p/mV	$\bar{E}^a$/V	$i_p^{ox}/\sqrt{v}c^{0\,b}$	i_p^{red}/i_p^{ox}
0.21	0.01	0.991	0.925	66	0.958	45.9	0.59
	0.02	0.996	0.924	72	0.960	42.7	0.72
	0.05	0.992	0.929	63	0.961	41.1	0.72
	0.1	0.987	0.926	61	0.957	33.8	0.91
	0.2	0.987	0.927	60	0.957	33.2	0.96
	0.5	0.988	0.926	62	0.957	32.6	1.04
	1.0	0.987	0.927	60	0.957	37.6	0.96
	2.0	0.998	0.925	64	0.957	—	—
	5.0	0.994	0.930	64	0.962	—	—
	10.0	0.993	0.923	70	0.958	—	—
0.28	0.01	0.997	0.926	71	0.962	43.0	0.62
	0.02	0.996	0.924	72	0.960	41.1	0.78
	0.05	0.994	0.926	68	0.960	38.9	0.82
	0.1	0.989	0.929	60	0.959	37.6	0.87
	0.2	0.991	0.928	63	0.960	37.6	0.88
	0.5	0.991	0.929	62	0.960	32.6	1.07
	1.0	0.987	0.932	55	0.960	34.8	1.07
	2.0	0.990	0.926	64	0.958	—	—
	5.0	0.996	0.926	70	0.961	—	—
	10.0	0.996	0.924	72	0.960	—	—
mean		0.992 ± 0.003	0.927 ± 0.002	65 ± 5	0.959 ± 0.002	35.0 ± 2.2[c]	—

[a] Midpoint potential $\bar{E} = (E_p^{ox} + E_p^{red})/2$. [b] In A cm^3 s$^{1/2}$ V$^{-1/2}$ mol^{-1}. [c] From values for $v > 50$ mV s^{-1}.

provide direct quantitative measures of the standard deviations of the parameter values estimated by fitting. Consequently, no further analysis is possible.

The heterogeneous electron transfer rate constant determined by the fitting procedure for the oxidation of $B_8Cl_8^{\bullet -}$ is still rather close to the reversibility/quasireversibility border. The characteristic changes in the shapes of the voltammograms at slow scan rates allow the determination of the rate of the homogeneous redox process (Table 7). Its value is similar for both clusters.

Thus, simulation of these voltammograms confirms the reaction mechanism proposed and the system parameters derived from the peak features and chronocoulograms. Furthermore, it allows determination of the rate constants of the homogeneous redox processes under the assumption of first-order kinetics.

Formal potentials and stability of the radical anions $B_nCl_n^{\bullet -}$

In previous paragraphs we have shown that both the reduction and (at large scan rates) the oxidation of $B_9Cl_9^{\bullet -}$ and $B_8Cl_8^{\bullet -}$ are chemically reversible processes with rates of the electron transfers close to or in the region of electrochemical reversibility. Under such conditions and under the assumption of equal diffusion coefficients for the three redox partners, respectively, the midpoint potentials, calculated as the mean values of the peak potentials, are good approximations for the formal potentials of the respective electron transfer processes. This is confirmed by the simulations which result in optimum E^0 values identical to the $\bar{E}$ within one standard deviation.

The formal potentials thus determined for the B_nCl_n systems in CH_2Cl_2 show a normal ordering, *i.e.* they increase with the oxidation state involved. The relative position of the E^0 for the redox processes of $B_9Cl_9^{\bullet -}$ is very similar in CH_2Cl_2 ($|\Delta E^0| = 0.533$, this work; 0.51;[38] 0.53 V[39]) and CH_3CN ($|\Delta E^0| = 0.540$ V[37]). On the other hand, the absolute values determined here and in the work of other authors are not comparable due to the use of different reference standards and the possibility of effects of the halogenated substrates on the potential of the Ag–AgCl electrode used in the earlier work.[37,38] If indeed the cluster radical anions are produced by hydrolysis of some of the

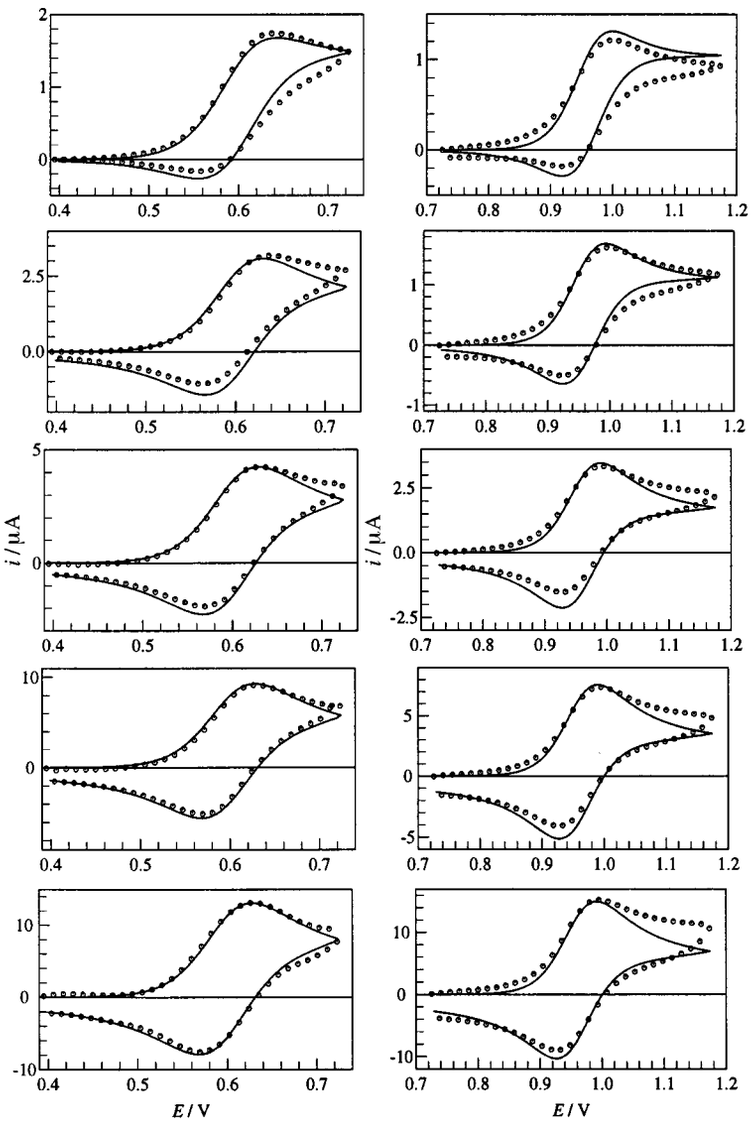

Fig. 8 Simulated (solid lines) and experimental (dots) cyclic voltammograms for the oxidation processes of $B_9Cl_9^{\bullet -}$ (left; $c^0 = 0.98$ mM, GC, $v = 0.01, 0.05, 0.1, 0.5, 1.0$ V s^{-1}, from top to bottom) and $B_8Cl_8^{\bullet -}$ (right; $c^0 = 0.28$ mM, Pt, $v = 0.01, 0.02, 0.1, 0.5, 2.0$ V s^{-1}).

Table 7 System parameter[a] sets for simulations of the process $B_nCl_n^{\bullet -} - e^- \rightleftharpoons B_nCl_n$

Parameter	$n = 9$	$n = 8$
E^0/V	+0.600	+0.959
D/cm^2 s^{-1}	6×10^{-7}	5.5×10^{-6}
k_s/cm s^{-1}	—[b]	0.13
α	0.5	0.5
k/s^{-1}	0.09	0.07

[a] Parameters describing the details of the mechanistic reaction steps.[49] [b] Electron transfer fully diffusion controlled.

subhalide molecules, as formulated in eqns. (7) and (8), chloride ions are liberated which will shift the reference potential. Our reference system should not be affected by such processes. Only the data in ref. 39 ($E_1^0 = +0.10$ V and $E_2^0 + 0.63$ V *vs.* Fc/Fc$^+$) seem to have been determined with careful exclusion of such effects. They differ from our values by less than 40 mV.

From the formal potentials the equilibrium constants K_{comp} of reaction (4) follow through eqn. (5) as 1.1×10^9 ($n = 9$, in close agreement with $K_{comp} = 1.2 \times 10^9$ in ref. 39) and 1.9×10^{14} ($n = 8$). Both equilibria are strongly shifted to the side of the radical anions, which are thus rather stable with respect to disproportionation. Results for the B_9Br_9,[37–39] B_9I_9,[37,39] and $B_{10}Cl_{10}$[37] systems show a similar picture. It appears that the smaller cluster radical anion is even more stable in this respect than $B_9Cl_9^{\bullet -}$.

Conclusion

The electrochemical investigation of two electron hyperdeficient boron subhalides shows that both B_9Cl_9 and B_8Cl_8 and their respective radical anions and dianions can be interconverted at an electrode in a dichloromethane electrolyte through one-electron processes, well separated in potential. The reduction of the neutral clusters to the radical anions proceeds at rather positive potentials at the electrode, and additionally spontaneously with an electrolyte component.

In view of the hypothetical rationalization of the "potential inversion"[6] phenomenon, the stepwise manner of electron transfer in the clusters investigated nicely mirrors the fact that probably all oxidation states attain the deltahedral *closo* type structure without drastic geometrical changes accompanying the redox process.

Possibly, more pronounced structural rearrangements would be noticeable in smaller clusters of this series, such as the tetrahedral B_4Cl_4, where chemical reduction with trimethylstannane leads to the butterfly-shaped *arachno*-B_4H_{10}.[44] However, reduction of B_4Cl_4 without simultaneous transfer of hydrogen has not yet been observed. It is thus planned to investigate the

electrochemical reduction of such boron subhalide clusters of smaller size in future work.

Experimental

Solvents and supporting electrolyte

Dichloromethane (Burdick & Jackson) was distilled to separate the stabilizing cyclohexene and dried by standing for several hours over activated basic Al_2O_3 (activation procedure: 4 h at a temperature of 400 °C and a pressure of 2×10^{-3} mbar). Tetra-*n*-butylammonium hexafluorophosphate, NBu_4PF_6, was prepared from NBu_4Br and NH_4PF_6 (Fluka) as described before.[55] It was used in a concentration of 0.1 M. The electrolyte was degassed by three freeze–pump–thaw cycles before transferring it into the electrochemical cell under argon. Carbon tetrachloride (p.a., Merck) and the deuteriated solvents were dried over molecular sieves; NBu_4I (puriss.) was purchased from Fluka.

Syntheses

The synthesis and all manipulations of the chloroboranes B_8Cl_8 and B_9Cl_9 were carried out by using standard high-vacuum or inert-atmosphere techniques as described by Shriver and Drezdzon.[56] The compound B_2Cl_4 was obtained by the reaction of BCl_3 with copper vapor[57] and purified by fractional condensation until it showed a vapor pressure of 59 mbar at 0 °C.

Nonachlorononaborane(9). The compound B_9Cl_9 was prepared by heating B_2Cl_4 at 450 °C for 5 min under vacuum according to the procedure reported by Morrison.[44,58] The product was purified by fractional sublimation into a long glass tube connected to a high-vacuum line.

Octachlorooctaborane(8). The compound B_8Cl_8 was prepared similar to the synthesis described by Morrison.[44,59] In a typical experiment, a solution of 3.7 g B_2Cl_4 (22.6 mmol) in 12.5 g of CCl_4 was heated in a 100 ml flask under argon at 95 °C for 14 d. After evaporation of all volatile material (BCl_3, B_2Cl_4, CCl_4) at 0 °C (10^{-4} mbar) a black residue remained, which contained, according to the ^{11}B NMR spectrum, B_8Cl_8 (δ 64.8 in $CDCl_3$, 93 mol%), B_9Cl_9 (δ 58.2, approximately 7 mol%), as well as traces of $B_{10}Cl_{10}$ ($\delta^{11}B$ 63.2, *cf*. ref. 44; 63.5) and an unidentified boron compound with $\delta^{11}B$ 51.7. The compound B_8Cl_8 was separated from the reaction mixture and purified by fractionated sublimation under vacuum (10^{-4} mbar). Yield: 100 mg (0.27 mmol, 10% based upon B_2Cl_4). It should be noted that thick layers of B_8Cl_8 are nearly black, whereas thin layers look dark green and become purple upon contact with traces of air.

Electrochemical experiments

All electrochemical experiments were performed with a Bioanalytical Systems (BAS, West Lafayette, IN, USA) 100 B/W electrochemical workstation controlled by a standard 80486 processor based personal computer (control program version 2.0). For electroanalytical experiments a BAS platinum or glassy carbon electrode tip was used as the working electrode. The electroactive area of the disks was determined from cyclic voltammograms, chronoamperograms, and chronocoulograms of ferrocene in dichloromethane under the assumption of a diffusion coefficient $D(Fc) = 2.32 \times 10^{-5}$ cm^2 s^{-1}.[60] The counter electrode was a platinum wire (diameter: 1 mm). A Haber–Luggin double reference electrode[61] was used. The resulting potential values refer to Ag–Ag^+ (0.01 M in CH_3CN–0.1 M NBu_4PF_6). Ferrocene was used as an external standard.[62] Its potential was determined by separate cyclic voltammetric experiments in CH_2Cl_2. All potentials reported in this paper are rescaled to $E^0(Fc–Fc^+) = +0.226$ V (*vs*. the Ag–Ag^+ reference) and thus given *vs*. the Fc–Fc^+ redox potential.

For cyclic voltammetry, chronoamperometry and chronocoulometry a gas-tight full-glass three-electrode cell as described before[55] was used. It was purged with argon before being filled with the electrolyte. Background curves were recorded before adding the substrate to the electrolyte. The background currents were later subtracted from the experimental data measured in the presence of substrate. The uncompensated resistance in the cell was determined by the built-in procedure of the BAS 100 B/W instrument. For each scan rate a series of cyclic voltammograms was recorded with 70, 80, and 90% feed-back compensation of the *iR* drop. This was repeated for at least a second concentration in the same cell set-up. The resulting current–potential curves were compared and optimum compensation was assumed if the peak potential separation did not increase with concentration.

The instability of the boron subhalides with respect to oxygen and traces of water required special precautions during weighing of the compounds and transfer of the samples to the electrochemical cell. Weighing was performed under argon. A concentrated stock solution was prepared with the degassed electrolyte and defined volumes of this solution were added to the blank electrolyte in the cell. After registration of all necessary voltammograms and chronocoulograms, further portions of the stock solution were added without changing the electrode arrangement. In this way at least two series of curves were recorded in each experiment with different concentrations but otherwise identical conditions.

For electrolysis experiments (bulk electrolysis), working and counter electrodes were Pt/Ir 90/10 nets (Degussa, Hanau, Germany), separated by a glass frit. The bulk electrolysis cell was also gas-tight and its temperature was controlled to be 17 °C. It was purged with argon prior to being filled with electrolyte.

Rest potential measurements were performed using the standard experimental protocol of the BAS 100 B/W electrochemical workstation.

Data analysis and simulations

Cyclic voltammetric and chronocoulometric data were background corrected and evaluated with the BAS 100 B/W control program. Peak current ratios were determined according to Nicholson's procedure.[63] All error measures given in this paper are standard deviations. For simulations of the cyclic voltammograms the commercial simulator DigiSim[64] (Version 2.0) was used with standard numerical options.

ESR and NMR spectra

A Bruker ESP 300 spectrometer was used to record the ESR spectra. Preparation of the solution was similar to that for the electroanalytical experiments. Spectra were taken at various times after dissolution. For the determination of the *g* values the spectrometer was calibrated with Bruker "strong pitch" of $g = 2.0028$. The ^{11}B NMR spectra at 80.25 MHz were obtained on a Bruker WM 250 spectrometer. All ^{11}B NMR chemical shifts are referred to external $F_3B{\cdot}OEt_2$ in $CDCl_3$ or CD_2Cl_2, respectively.

Investigation of B_8Cl_8 and $NBu_4^+B_8Cl_8^{\cdot -}$ solutions. Solutions of B_8Cl_8 in $CDCl_3$ or CCl_4 were prepared by condensing the solvent (which was dried before with molecular sieves) onto B_8Cl_8 under vacuum. The solution was transferred under argon with a syringe to an NMR tube equipped with a polytetrafluoroethylene (PTFE) valve. For the ESR measurements, B_8Cl_8 and the purified and dried solvent ($CDCl_3$ or CH_2Cl_2) were condensed under vacuum into an ESR glass tube equipped with a PTFE valve or the components were condensed together in a flask connected to the vacuum line and transferred under argon with a syringe into the ESR tube. The $NBu_4^+B_8Cl_8^{\cdot -}$ was

prepared according to the synthesis of $NBu_4^+B_9Cl_9^{\bullet -}$[35] by reduction of B_8Cl_8 with the equivalent amount of NBu_4I in dried $CDCl_3$.

Acknowledgements

The authors thank Paul Schuler for recording the ESR spectra, Stefan Dümmling for technical assistance and the Fonds der Chemischen Industrie, Frankfurt/Main, Germany, for financial support.

References

1 B. Speiser and S. Dümmling, Part 1: *DECHEMA-Monogr.*, in the press.
2 K. Deuchert and S. Hünig, *Angew. Chem.*, 1978, **90**, 927; *Angew. Chem., Int. Ed. Engl.*, 1978, **17**, 875.
3 N. G. Connelly and W. E. Geiger, *Adv. Organomet. Chem.*, 1984, **23**, 1.
4 J. Phelps and A. J. Bard, *J. Electroanal. Chem. Interfacial Electrochem.*, 1976, **68**, 313.
5 D. H. Evans, *Acta Chem. Scand.*, 1998, **52**, 194.
6 D. H. Evans and K. Hu, *J. Chem. Soc., Faraday Trans.*, 1996, 3983.
7 K. Hu and D. H. Evans, *J. Electroanal. Chem. Interfacial Electrochem.*, 1997, **423**, 29.
8 K. Hu, M. E. Niyazymbetov and D. H. Evans, *J. Electroanal. Chem. Interfacial Electrochem.*, 1995, **396**, 457.
9 K. Hu and D. H. Evans, *J. Phys. Chem.*, 1996, **100**, 3030.
10 B. Speiser, M. Würde and C. Maichle-Mössmer, *Chem. Eur. J.*, 1998, **4**, 222.
11 B. Tulyathan and W. E. Geiger, *J. Am. Chem. Soc.*, 1985, **107**, 5960.
12 J. A. Morrison, in *Advances in Boron and the Boranes*, eds. J. F. Liebman, A. Greenberg, R. E. Williams, D. P. Loker and K. B. Loker, VCH, Weinheim, 1988, vol. 5, ch. 8, pp. 151–189.
13 R. L. Johnston and D. M. P. Mingos, *Inorg. Chem.*, 1986, **25**, 3321.
14 K. Wade, *Adv. Inorg. Chem. Radiochem.*, 1976, **18**, 1.
15 R. A. Jacobson and W. N. Lipscomb, *J. Am. Chem. Soc.*, 1958, **80**, 5571.
16 M. Atoji and W. N. Lipscomb, *J. Chem. Phys.*, 1959, **31**, 601.
17 R. A. Jacobson and W. N. Lipscomb, *J. Chem. Phys.*, 1959, **31**, 605.
18 L. J. Guggenberger, *Inorg. Chem.*, 1969, **8**, 2771.
19 W. Hönle, Y. Grin, A. Burkhardt, U. Wedig, M. Schultheiss, H. G. von Schnering, R. Kellner and H. Binder, *J. Solid State Chem.*, 1997, **113**, 59.
20 M. B. Hursthouse, J. Kane and A. G. Massey, *Nature* (*London*), 1970, **228**, 659.
21 L. J. Guggenberger, *Inorg. Chem.*, 1969, **7**, 2260.
22 J. Thesing, J. Baurmeister, W. Preetz, D. Thiery and H. G. von Schnering, *Z. Naturforsch., Teil B*, 1991, **46**, 800.
23 W. Preetz and J. Fritze, *Z. Naturforsch., Teil B*, 1984, **39**, 1472.
24 A. Heinrich, H.-L. Keller and W. Preetz, *Z. Naturforsch., Teil B*, 1990, **45**, 184.
25 R. Schaeffer, Q. Johnson and G. S. Smith, *Inorg. Chem.*, 1965, **4**, 917.
26 M. L. McKee, *Inorg. Chem.*, 1999, **38**, 321.
27 M. Atoji and W. N. Lipscomb, *Acta Crystallogr.*, 1953, **6**, 547.
28 M. J. S. Dewar and M. L. McKee, *Inorg. Chem.*, 1978, **17**, 1569.
29 A. Neu, T. Mennekes, U. Englert, P. Paetzold, M. Hofmann and P. von R. Schleyer, *Angew. Chem.*, 1997, **1094**, 2211; *Angew. Chem., Int. Ed. Engl.*, 1997, **36**, 2117.
30 M. E. O'Neill and K. Wade, *Inorg. Chem.*, 1982, **21**, 461.
31 M. E. O'Neill and K. Wade, *J. Mol. Struct.*, 1983, **103**, 259.
32 M. A. Fox and K. Wade, in *The Borane, Carborane, Carbocation Continuum*, ed. J. Casanova, Wiley, New York, 1998, ch. 2, pp. 62–64.
33 R. W. Rudolph and W. R. Pretzer, *Inorg. Chem.*, 1972, **11**, 1974.
34 D. A. Kleier and W. N. Lipscomb, *Inorg. Chem.*, 1979, **18**, 1312.
35 E. H. Wong and R. M. Kabbani, *Inorg. Chem.*, 1980, **19**, 451.
36 F. Klanberg, D. R. Eaton, L. J. Guggenberger and E. L. Muetterties, *Inorg. Chem.*, 1967, **6**, 1271.
37 W. Bowden, *J. Electrochem. Soc.*, 1982, **129**, 1249.
38 R. Kellner, Ph.D. Thesis, Universität Stuttgart, 1997.
39 H. Binder, R. Kellner, K. Vaas, M. Hein, F. Baumann, M. Wanner, R. Winter, W. Kaim, W. Hönle, Y. Grin, U. Wedig, M. Schulthesis, R. K. Kremer, H. G. von Schnering, O. Groeger and G. Engelhardt, personal communication.
40 G. F. Lanthier and A. G. Massey, *J. Inorg. Nucl. Chem.*, 1970, **32**, 1807.
41 G. F. Lanthier, J. Kane and A. G. Massey, *J. Inorg. Nucl. Chem.*, 1971, **33**, 1569.
42 E. H. Wong, *Inorg. Chem.*, 1981, **20**, 1300.
43 E. P. Schram and G. Urry, *Inorg. Chem.*, 1963, **2**, 405.
44 J. A. Morrison, *Chem. Rev.*, 1991, **91**, 35.
45 S. L. Emery, Ph.D. Thesis, University of Illinois, Chicago, 1985.
46 R. S. Nicholson and I. Shain, *Anal. Chem.*, 1964, **36**, 706.
47 F. C. Anson, *Anal. Chem.*, 1966, **38**, 54.
48 A. J. Bard and L. R. Faulkner, *Electrochemical Methods. Fundamentals and Applications*, Wiley, New York, 1980, p. 201 ff.
49 B. Speiser, *Anal. Chem.*, 1985, **57**, 1390.
50 J. Heinze, *Angew. Chem.*, 1984, **96**, 823; *Angew. Chem., Int. Ed. Engl.*, 1984, **23**, 831.
51 J. M. Savéant and E. Vianello, *Adv. Polarography*, 1960, **2**, 367.
52 J. M. Savéant and E. Vianello, *Electrochim. Acta*, 1965, **10**, 905.
53 L. K. Bieniasz and B. Speiser, *J. Electroanal. Chem.*, 1998, **441**, 271.
54 L. K. Bieniasz and B. Speiser, *J. Electroanal. Chem.*, 1998, **458**, 209.
55 S. Dümmling, E. Eichhorn, S. Schneider, B. Speiser and M. Würde, *Curr. Sep.*, 1996, **15**, 53.
56 D. F. Shriver and M. A. Drezdzon, *The Manipulation of Air-Sensitive Compounds*, 2nd edn., Wiley, New York, 1986.
57 P. L. Timms, *Adv. Inorg. Chem. Radiochem.*, 1972, **14**, 121.
58 T. Davan and J. A. Morrison, *Inorg. Chem.*, 1986, **25**, 2366.
59 S. L. Emery and J. A. Morrison, *J. Am. Chem. Soc.*, 1982, **104**, 6790.
60 J. B. Cooper and A. M. Bond, *J. Electroanal. Chem. Interfacial Electrochem.*, 1991, **315**, 143.
61 B. Gollas, B. Krauß, B. Speiser and H. Stahl, *Curr. Sep.*, 1994, **13**, 42.
62 G. Gritzner and J. Kůta, *Pure Appl. Chem.*, 1984, **56**, 461.
63 R. S. Nicholson, *Anal. Chem.*, 1966, **38**, 1406.
64 M. Rudolph, D. P. Reddy and S. W. Feldberg, *Anal. Chem.*, 1994, **66**, 589A.

Paper 8/09134J